Multiplex Detection

DOI: 10.1002/anie.201401026

Plasmonic Liquid Marbles: A Miniature Substrate-less SERS Platform for Quantitative and Multiplex Ultratrace Molecular Detection**

*Hiang Kwee Lee, Yih Hong Lee, In Yee Phang, Jiaqi Wei, Yue-E Miao, Tianxi Liu, and Xing Yi Ling**

Abstract: *Inspired by aphids, liquid marbles have been studied extensively and have found application as isolated microreactors, as micropumps, and in sensing. However, current liquid-marble-based sensing methodologies are limited to qualitative colorimetry-based detection. Herein we describe the fabrication of a plasmonic liquid marble as a substrate-less analytical platform which, when coupled with ultrasensitive SERS, enables simultaneous multiplex quantification and the identification of ultratrace analytes across separate phases. Our plasmonic liquid marble demonstrates excellent mechanical stability and is suitable for the quantitative examination of ultratrace analytes, with detection limits as low as 0.3 fmol, which corresponds to an analytical enhancement factor of* 5×10^8*. The results of our simultaneous detection scheme based on plasmonic liquid marbles and an aqueous–solid–organic interface quantitatively tally with those found for the individual detection of methylene blue and coumarin.*

Aphids encapsulate their excreted liquid waste within a thin layer of wax to form sphere-like structures, known as "liquid marbles", to prevent the flooding of their colony.[1] Inspired by the natural process of transforming liquids into "soft" solids with enhanced mobility, extensive research on liquid marbles fabricated by the spontaneous encapsulation of water droplets with pulverized hydrophobic micro- or nanoparticles has been undertaken during the past decade.[2] The encapsulating hydrophobic particles impart strong water-repelling properties on the liquid marbles to prevent any interaction of the water droplet with the underlying platform, thus giving liquid marbles a unique non-stick behavior.[3] Given the flexibility in the choice of solid particles to form liquid marbles and their excellent mechanical robustness, it is no surprise that liquid marbles are fast emerging as an alternative substrate-less platform.[4] Various applications exploiting the superhydrophobicity (contact angle $\geq 150°$) of liquid marbles and their ability to isolate small-volume liquids[5] have been reported, including controlled transportation in a microfluidic system,[6] their use as isolated microreactors,[7] as micropumps,[8] and in sensing.[9]

Liquid marbles offer tremendous potential as miniaturized and substrate-less sensing platforms for trace-analyte detection. Although there have been reports of the application of liquid marbles for qualitative colorimetry-based detection,[9] no study on the quantitative spectroscopic sensing of trace analytes has been conducted. We envisage the use of a combination of plasmonic liquid marbles, formed by using metallic (Ag or Au) nanoparticles, with surface-enhanced Raman spectroscopy (SERS) as an attractive ensemble to produce a substrate-less analytical platform to enable the simultaneous quantification and identification of target analytes.

Typically, conventional SERS sensors are fabricated by the assembly of Ag/Au nanoparticles on solid substrates.[10] These substrate-based platforms have demonstrated 10^4- to 10^{12}-fold enhancement of Raman signals,[11] thus providing molecular fingerprints even for femto-/attomolar detection.[12] This behavior can be attributed to the intense electromagnetic fields generated by the incident excitation of localized surface plasmon resonances (LSPRs) of the plasmonic nanoparticles.[13] However, substrate-based SERS sensors are limited by their need for multistep fabrication, and sequential protocols are required for multiplex analysis involving different phases. Even though there have been reports on the use of nanoparticle monolayers assembled at liquid–liquid or liquid–air interfaces for the simultaneous substrate-less detection of multiple analytes across interfaces,[14] this approach generally lacks robustness, as the nanoparticle assembly is prone to disruption from thermal/physical agitation, which ultimately affects the SERS signal. Hence, the synergy of miniaturized, mechanically stable, readily prepared plasmonic liquid marbles with ultrasensitive SERS is immensely promising in terms of both the quantification and identification of trace analytes and also the multiplex simultaneous detection of analytes in separate phases. The application of plasmonic liquid marbles as an analytical platform therefore offers great versatility and time efficiency for the detection of samples involving multiple analytes and/or phases, as are commonly observed in industrial discharge and polluted water.

[*] H. K. Lee, Dr. Y. H. Lee, J. Wei, Prof. X. Y. Ling
Division of Chemistry and Biological Chemistry, School of Physical and Mathematical Sciences, Nanyang Technological University
50 Nanyang Ave, Singapore 637371 (Singapore)
E-mail: xyling@ntu.edu.sg
Dr. I. Y. Phang
Institute of Materials Research and Engineering
A*STAR (Agency for Science, Technology and Research)
3 Research Link, Singapore 117602 (Singapore)
Y. Miao, Prof. T. Liu
State Key Laboratory of Molecular Engineering of Polymers
Department of Macromolecular Science, Fudan University
Shanghai 200433 (P.R. China)

[**] X.Y.L. thanks the National Research Foundation, Singapore (NRF-NRFF2012-04) for support and Nanyang Technological University for a start-up grant. H.K.L. thanks A*STAR, Singapore for an A*STAR Graduate Scholarship. SERS = surface-enhanced Raman spectroscopy.

Supporting information for this article is available on the WWW under http://dx.doi.org/10.1002/anie.201401026.

Herein, we demonstrate the fabrication of silver-nanoparticle-based plasmonic liquid marbles and their application as a substrate-less SERS platform for multiplex and quantitative ultratrace molecular detection.[15] We use single-crystalline Ag nanocubes as the encapsulating hydrophobic powder for liquid-marble formation. The physical properties of the plasmonic liquid marbles, especially their mechanical stability and robustness as mobile, superhydrophobic platforms, are demonstrated. By using SERS as the detection technique, we find that these plasmonic liquid marbles are capable of ultratrace molecular sensing down to the femtomole level. The ability of the plasmonic liquid marbles to sense ultratrace analytes in a single phase (aqueous or organic) and also simultaneously across the oil/water interface is examined.

Single-crystalline Ag nanocubes are chosen as the building blocks for the formation of plasmonic liquid marbles, as their well-defined edges/tips can generate intense localized electromagnetic fields for SERS enhancement upon excitation by a laser in the visible region (see Figure S1 in the Supporting Information). Furthermore, Ag nanocubes can be synthesized in high yield by the polyol route:[16] Approximately 40 mg of dried Ag nanocube powder can be produced per synthesis, which enables the formation of multiple plasmonic liquid marbles. The Ag nanocubes exhibit excellent monodispersity, with an average edge length of (125 ± 5) nm (Figure 1 A; see also Figure S1 A,B in the Supporting Information).

To confer hydrophobicity to the Ag nanocubes, the as-synthesized poly(vinylpyrrolidone)-capped Ag nanocubes are first functionalized with 1*H*,1*H*,2H,2*H*-perfluorodecanethiol (PFDT) and subsequently dried and pulverized to yield the hydrophobic Ag nanocube powder (Figure 1 B). The perfluorodecanethiol-grafted Ag nanocubes exhibit excellent anti-wetting properties (water contact angle: $(153 \pm 5)°$); in contrast, as a powder, poly(vinylpyrrolidone)-capped Ag nanocubes undergo rapid wetting by water (see Figure S2). This comparison clearly emphasizes the need to graft hydrophobic moieties onto the Ag nanocubes to impart hydrophobicity, which is essential for subsequent liquid-marble formation (see the Supporting Information for the characterization of other Ag nanocube powders.

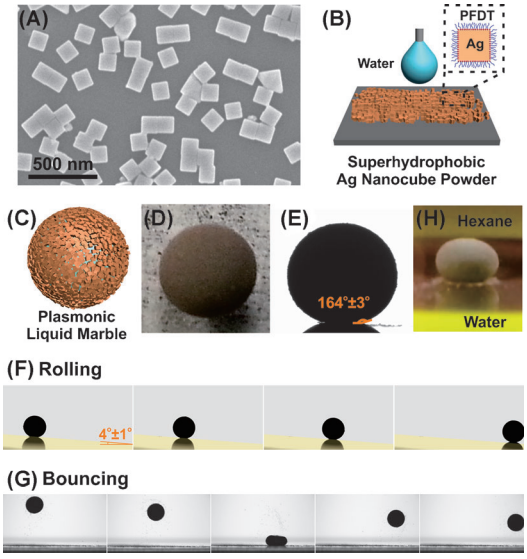

Figure 1. Fabrication and characterization of plasmonic liquid marbles. A) SEM image of as-synthesized Ag nanocubes. B) A plasmonic liquid marble is formed by placing a 3 μL water droplet on perfluorodecanethiol-functionalized Ag nanocubes. C) Illustration of a liquid marble formed by using Ag nanocubes. D) Digital photographic image of a plasmonic liquid marble. E) Contact angle of the same plasmonic liquid marble. F) Rolling and G) bouncing of a plasmonic liquid marble (from left to right). H) Submersion and floating of a plasmonic liquid marble in hexane and on water (yellow layer), respectively.

Plasmonic liquid marbles are formed by rolling a 3 μL water droplet over a bed of the hydrophobic Ag nanocube powder (Figure 1 C); the resulting plasmonic liquid marble appears dull grayish-green owing to the diffuse scattering of light from the powder (Figure 1 D). The static contact angle of the plasmonic liquid marble as measured on a hydrophilic glass coverslip is $(164 \pm 3)°$ (Figure 1 E) and indicates minimal interaction between the plasmonic liquid marble and the solid surface. The amount of Ag nanocube powder required to form a single plasmonic liquid marble is estimated to be approximately 0.18 mg by gravimetric analysis and corresponds to a powder thickness of around 1.7 μm or 13 layers of Ag nanocubes (see the Supporting Information for more details).

The plasmonic liquid marble is then subjected to various mechanical tests, including rolling and bouncing, to evaluate its suitability as a substrate-less analytical platform for interfacial applications. The plasmonic liquid marble demonstrates excellent non-stick properties with lotus-like behavior, whereby a slip-off angle of $(4 \pm 1)°$ is observed (Figure 1 F). The plasmonic liquid marble is also mechanically stable and does not break even when dropped from a height of 1 cm (Figure 1 G). Furthermore, the plasmonic liquid marble can be submerged in some liquids and float on others, thus highlighting its suitability for interfacial applications (Figure 1 H). The mechanical characterization studies collectively demonstrate the mechanical robustness of our plasmonic liquid marble as a substrate-less system and also its suitability for interfacial applications (see the Supporting Information for more details).

To identify the SERS-active areas on the plasmonic liquid marbles, we perform *x*–*y* and *x*–*z* hyperspectral SERS imaging on the 3 μL plasmonic liquid marbles encapsulating methylene blue (0.3 nmol) submerged in hexane (Figure 2 A). The SERS spectrum obtained exhibits the characteristic vibrational modes of methylene blue (Figure 2 C; see Table S1 in the Supporting Information for assignment). The *x*–*y* SERS image overlaid with its optical microscopic image (Figure 2 B) shows that the edges of the plasmonic liquid marbles are brightly lit when the most intense C=C ring stretching mode of methylene blue at 1634 cm^{-1} is selected. A waterfall plot of the SERS spectra in the *x*–*y* plane (Figure 2 C) from the interior (I) to the exterior (II) of the plasmonic liquid marble further indicates that the strongest signals ((4347 ± 453) counts/s) are recorded along the edges of the liquid marble, where the Ag nanocube powder is located. In areas away from the Ag nanocube powder, SERS intensities average around (505 ± 29) counts/s in the interior

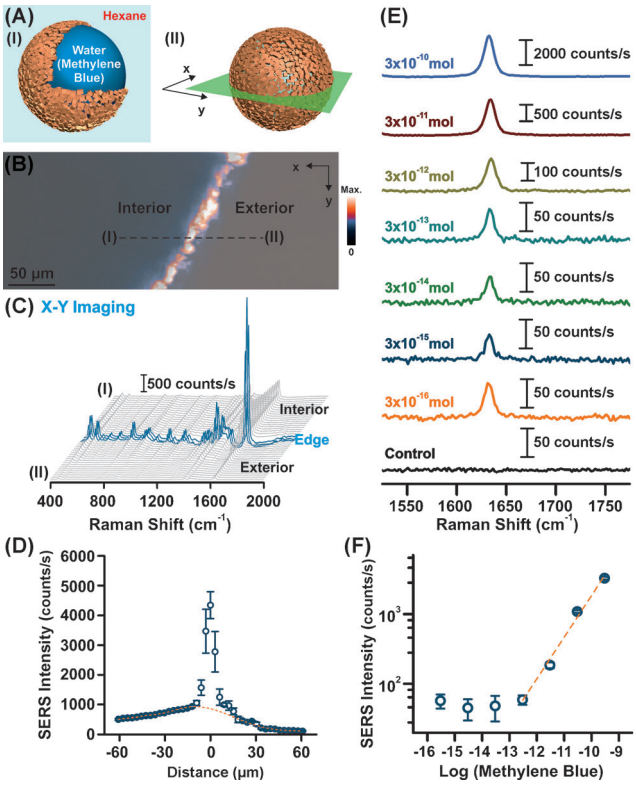

Figure 2. Characterization of the SERS-active areas and SERS sensing capabilities of plasmonic liquid marbles by using methylene blue encapsulated within the marble. A) Illustration of I) SERS detection of the encapsulated aqueous methylene blue and II) *x*–*y* SERS imaging on a plasmonic liquid marble. B) Overlay of the *x*–*y* SERS image of a plasmonic liquid marble containing methylene blue (0.3 nmol) with its optical image. The black dotted line denotes the location at which the SERS intensity line profile is obtained. C) SERS spectrum and D) SERS intensity profiling along the black dotted line in (B). Negative and positive distances correspond to the interior and exterior of the liquid marble, respectively, with the edge defined as distance = 0 μm. E) SERS spectra and F) SERS intensity for methylene blue at concentrations ranging from 0.3 fmol to 0.3 nmol. "Control" refers to SERS analysis on a plasmonic liquid marble without methylene blue.

of the plasmonic liquid marble, whereas negligible signals of (115 ± 25) counts/s are recorded at the exterior of the plasmonic liquid marble (Figure 2D). Similarly, maximum SERS intensity is also observed at the edge in the *x*–*z* SERS image (see the Supporting Information for a more detailed discussion on the *x*–*z* SERS image and comparison with the *x*–*y* SERS image). The strong SERS intensities at the edge of the liquid marble are expected, as SERS is a surface analytical method in which the electromagnetic enhancement decays exponentially with increasing separation between the analyte and the surface of Ag nanocubes.[17] The SERS intensity line profiles for both *x*–*y* and *x*–*z* imaging therefore hint at the suitability of the entire plasmonic liquid marble edge for molecular sensing. From this point onwards we always use *x*–*y* SERS imaging, as there is less interference than that observed for *x*–*z* imaging, and only SERS spectra at the edge of plasmonic liquid marbles are discussed.

We characterize the SERS responses of our plasmonic liquid marbles in three scenarios, namely, for: 1) an analyte within the encapsulated aqueous phase, 2) an analyte outside of the liquid marble, in the organic phase, and 3) analytes in both the interior aqueous phase and the exterior organic phase. Methylene blue and coumarin are used as the probe analytes for the aqueous and organic phase, respectively. Quantitative SERS detection of methylene blue encapsulated within the 3 μL plasmonic liquid marble is conducted by loading various concentrations of the analyte molecules into the marble (Figure 2A, I). The magnified SERS spectra in the Raman shift window between 1550 and 1750 cm^{-1} for methylene blue (0.3 fmol–0.3 nmol) show that the detection limit of methylene blue is 0.3 fmol, for which a SERS intensity of (57 ± 13) counts/s with a signal-to-noise ratio higher than 3:1 is observed (Figure 2E). A plasmonic liquid marble in the absence of methylene blue gives a featureless SERS spectrum ("control" in Figure 2E), thus demonstrating that perfluorodecanethiol adsorbed on Ag nanocubes does not interfere with ultratrace sensing owing to the weak/moderate Raman response associated with the C–F group.[18] The correlation of SERS intensities with analyte concentration indicates a linear range from 0.3 pmol to 0.3 nmol (orange dotted line in Figure 2F). At lower concentrations between 0.3 fmol and 0.3 pmol, the SERS intensities remain relatively constant at approximately 50 counts/s. This behavior is attributed to the sub-monolayer Langmuir adsorption of analytes onto the Ag nanocube surfaces (see Figure S4). Furthermore, the analytical enhancement factor (AEF) of the plasmonic liquid marbles with methylene blue concentrations of 0.3 fmol is calculated to be 5×10^8 (see the Supporting Information for details on the AEF calculation). This value indicates that our system is able to provide an approximately 10^8-fold enhancement of Raman intensity relative to that observed in the absence of the encapsulating plasmonic Ag nanocube powder. This high AEF is mainly attributed to the presence of high SERS hotspot densities in the Ag nanocube powder, in which Ag nanocubes are closely packed together.[19]

Further to the quantitative ultratrace detection of an aqueous analyte encapsulated within the plasmonic liquid marble, the exterior of the plasmonic liquid marble can also be used for analyte detection in the organic phase (Figure 3A). Figure 3B shows a typical SERS spectrum of coumarin, an organic-soluble compound (see Table S2 for the assignment of the SERS bands). The variation in the SERS intensity of the most intense ring-stretching band at 780 cm^{-1} in the concentration range between 0.1 nmol and 1 μmol is shown in Figure 3C. The detection limit for coumarin in the organic phase is 0.1 nmol, with an average SERS intensity of (24 ± 11) counts/s. The linearity range is determined to be between 0.1 nmol and 1 μmol from the correlation plot of SERS intensity against the concentration of coumarin (orange dotted line in Figure 3D). The AEF based on coumarin is estimated to be 10^7 (see the Supporting Information for details), which is comparable to the AEF calculated by using methylene blue. The slight decrease in the analytical enhancement factor (by about one order of magnitude) for detection in the organic phase is probably due to the relative increase in background interference contributed by Raman-active organic solvent molecules (see

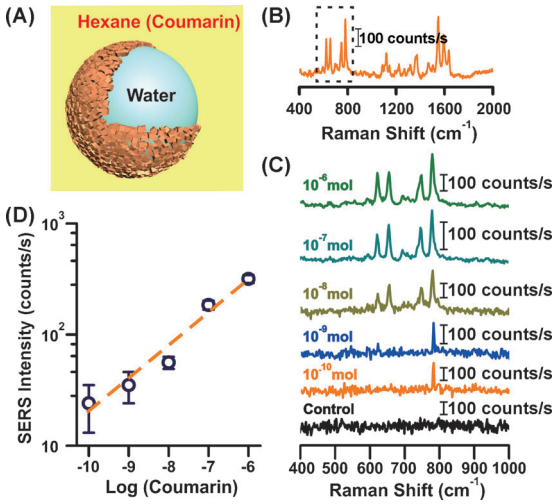

Figure 3. SERS sensing of coumarin in the organic phase outside the plasmonic liquid marble. A) Illustration of SERS detection of coumarin in the organic phase. B) SERS spectrum of coumarin. The black dotted box indicates the Raman shift window of interest. C) SERS spectra and D) SERS intensity for coumarin at concentrations ranging from 0.1 nmol to 1 μmol. "Control" refers to SERS analysis on a plasmonic liquid marble in the absence of coumarin.

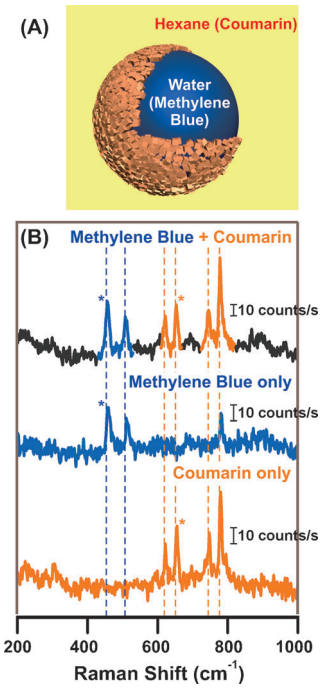

Figure 4. Multiplex interfacial SERS analysis of methylene blue (aqueous phase) and coumarin (organic phase) with plasmonic liquid marbles. A) Illustration of the SERS detection scheme. B) SERS spectrum for the multiplex interfacial detection of methylene blue and coumarin (top). Individual SERS spectra of methylene blue in the aqueous phase (middle) and coumarin in the organic phase (bottom) at the same respective concentrations are included for comparison.

Figure S6) at the highly diluted analyte concentration (<0.1 nmol). Nevertheless, the generally high AEF ($>10^7$) is a clear demonstration that the plasmonic liquid marble is able to provide strong signal enhancement on its Ag nanocube shell, both internally and externally, for sensing applications.

The capability of our plasmonic liquid marble for simultaneous ultratrace detection of both analytes across the liquid–solid–liquid interface is demonstrated in Figure 4. In this setup, methylene blue (3 pmol) is encapsulated within the marble, and coumarin (10 nmol) is present in the organic phase (Figure 4A). The SERS spectrum for the interfacial detection of methylene blue and coumarin shows fingerprint peaks corresponding to both probe molecules (Figure 4B). A comparison of this SERS spectrum with those for single-analyte detection shows that the blue peaks (457 and 508 cm^{-1}) can be explicitly indexed to methylene blue, whereas the orange peaks (622, 655, 747 and 780 cm^{-1}) can be assigned to coumarin. Importantly, the SERS intensities of the selected bands ((48 ± 7) and (42 ± 22) counts/s for 457 and 655 cm^{-1}, respectively) in the simultaneous detection scheme can be quantitatively tallied to the individual detection of both methylene blue and coumarin (see Figure S7), with accuracy up to one standard deviation. To the best of our knowledge, this interfacial detection technique is the first for which the SERS intensities of different analytes can be directly related for both simultaneous and individual detection. In contrast, with other methods based on the interfacial assembly of nanoparticles, only relative concentrations of the analytes can be resolved.[14] Hence, it is evident that the mechanical stability of our plasmonic liquid marble provides an analytical platform less prone to environmental interference with SERS signals. Thus, a reproducible SERS response across different plasmonic liquid marbles is possible, as well as the concurrent determination of multiple analytes with different concentrations in separate phases. Furthermore, this system is dynamically stable (the plasmonic liquid marble does not dry up quickly), and the rapid readout of SERS signals enables high signal reproducibility over the course of data collection without interference from solvent vaporization (see Figure S8).

In summary, we have introduced plasmonic liquid marbles as a substrate-less analytical platform for the simultaneous interfacial detection of multiple analytes. This process is facilitated by the mechanical robustness of the plasmonic liquid marbles, which are capable of rolling and bouncing, and remain stable in various solvents. The quantitative detection of individual analytes reaches femtomole levels for the aqueous-based detection of methylene blue and nanomole levels for the organic-phase detection of coumarin. Multiplex detection of these two analytes is also demonstrated at ultratrace levels. The protocol for the fabrication of plasmonic liquid marbles is also generic and can be extended to other nanoparticles or a combination of nanoparticles to tailor the plasmonic response and mechanical properties of the liquid marbles. The multiple advantages of plasmonic liquid marbles will enable them to find application in lab-on-a-chip systems for on-site ultratrace and/or quantitative sensing in various fields, such as industrial/environment safety, criminology, and antiterrorism.

Received: January 30, 2014
Published online: April 1, 2014

Keywords: liquid marbles · multiplex detection · sensors · surface-enhanced Raman spectroscopy · ultratrace detection

[1] N. Pike, D. Richard, W. Foster, L. Mahadevan, *Proc. R. Soc. London Ser. B* **2002**, *269*, 1211 – 1215.
[2] a) P. Aussillous, D. Quéré, *Nature* **2001**, *411*, 924 – 927; b) E. Bormashenko, *Soft Matter* **2012**, *8*, 11018 – 11021; c) D. Quéré, P. Aussillous, *Chem. Eng. Technol.* **2002**, *25*, 925 – 928.
[3] a) E. Bormashenko, Y. Bormashenko, A. Musin, Z. Barkay, *ChemPhysChem* **2009**, *10*, 654 – 656; b) E. Bormashenko, Y. Bormashenko, A. Musin, *J. Colloid Interface Sci.* **2009**, *333*, 419 – 421.
[4] a) E. Bormashenko, R. Pogreb, A. Musin, *J. Colloid Interface Sci.* **2012**, *366*, 196 – 199; b) D. Zang, Z. Chen, Y. Zhang, K. Lin, X. Geng, B. P. Binks, *Soft Matter* **2013**, *9*, 5067 – 5073; c) E. Bormashenko, Y. Bormashenko, G. Oleg, *Langmuir* **2010**, *26*, 12479 – 12482; d) E. Bormashenko, Y. Bormashenko, R. Pogreb, O. Gendelman, *Langmuir* **2010**, *26*, 7 – 10; e) E. Bormashenko, R. Pogreb, R. Balter, O. Gendelman, D. Aurbach, *Appl. Phys. Lett.* **2012**, *100*, 1516011; f) E. Bormashenko, R. Pogreb, T. Stein, G. Whyman, M. Schiffer, D. Aurbach, *J. Adhes. Sci. Technol.* **2011**, *25*, 1371 – 1377.
[5] N. J. Shirtcliffe, G. McHale, S. Atherton, M. I. Newton, *Adv. Colloid Interface Sci.* **2010**, *161*, 124 – 138.
[6] a) P. Aussillous, D. Quéré, *Proc. R. Soc. London Ser. A* **2006**, *462*, 973 – 999; b) E. Bormashenko, R. Pogreb, Y. Bormashenko, A. Musin, T. Stein, *Langmuir* **2008**, *24*, 12119 – 12122; c) M. I. Newton, D. L. Herbertson, S. J. Elliott, N. J. Shirtcliffe, G. McHale, *J. Phys. D* **2007**, *40*, 20 – 24.
[7] a) T. Arbatan, L. Li, J. Tian, W. Shen, *Adv. Healthcare Mater.* **2012**, *1*, 80 – 83; b) Y. Xue, H. Wang, Y. Zhao, L. Dai, L. Feng, X. Wang, T. Lin, *Adv. Mater.* **2010**, *22*, 4814 – 4818.
[8] E. Bormashenko, R. Balter, D. Aurbach, *Appl. Phys. Lett.* **2010**, *97*, 0919081 – 0919082.
[9] a) J. Tian, T. Arbatan, X. Li, W. Shen, *Chem. Eng. J.* **2010**, *165*, 347 – 353; b) S. Fujii, K. Aono, M. Suzaki, S. Hamasaki, S.-i. Yusa, Y. Nakamura, *Macromolecules* **2012**, *45*, 2863 – 2873; c) E. Bormashenko, A. Musin, *Appl. Surf. Sci.* **2009**, *255*, 6429 – 6431.
[10] a) A. Kim, S. J. Barcelo, R. S. Williams, Z. Li, *Anal. Chem.* **2012**, *84*, 9303 – 9309; b) M. Alba, N. Pazos-Perez, B. Vaz, P. Formentin, M. Tebbe, M. A. Correa-Duarte, P. Granero, J. Ferré-Borrull, R. Alvarez, J. Pallares, A. Fery, A. R. de Lera, L. F. Marsal, R. A. Alvarez-Puebla, *Angew. Chem.* **2013**, *125*, 6587 – 6591; *Angew. Chem. Int. Ed.* **2013**, *52*, 6459 – 6463; c) X. Wang, M. Li, L. Meng, K. Lin, J. Feng, T. Huang, Z. Yang, B. Ren, *ACS Nano* **2013**, *8*, 528 – 536; d) L. Polavarapu, L. M. Liz-Marzán, *Phys. Chem. Chem. Phys.* **2013**, *15*, 5288 – 5300.
[11] a) H. Ko, S. Singamaneni, V. V. Tsukruk, *Small* **2008**, *4*, 1576 – 1599; b) E. C. Le Ru, E. Blackie, M. Meyer, P. G. Etchegoin, *J. Phys. Chem. C* **2007**, *111*, 13794 – 13803; c) M.-W. Shao, L. Lu, H. Wang, S. Wang, M.-L. Zhang, D.-D.-D. Ma, S.-T. Lee, *Chem. Commun.* **2008**, 2310 – 2312.
[12] a) H. K. Lee, Y. H. Lee, Q. Zhang, I. Y. Phang, J. M. R. Tan, Y. Cui, X. Y. Ling, *ACS Appl. Mater. Interfaces* **2013**, *5*, 11409 – 11418; b) F. De Angelis, F. Gentile, F. Mecarini, G. Das, M. Moretti, P. Candeloro, M. L. Coluccio, G. Cojoc, A. Accardo, C. Liberale, R. P. Zaccaria, G. Perozziello, L. Tirinato, A. Toma, G. Cuda, R. Cingolani, E. Di Fabrizio, *Nat. Photonics* **2011**, *5*, 682 – 687; c) L.-Q. Lu, Y. Zheng, W.-G. Qu, H.-Q. Yu, A.-W. Xu, *J. Mater. Chem.* **2012**, *22*, 20986 – 20990.
[13] a) W. Knoll, *Annu. Rev. Phys. Chem.* **1998**, *49*, 569 – 638; b) K. L. Kelly, E. Coronado, L. L. Zhao, G. C. Schatz, *J. Phys. Chem. B* **2002**, *106*, 668 – 677.
[14] a) K. Kim, H. S. Han, I. Choi, C. Lee, S. Hong, S.-H. Suh, L. P. Lee, T. Kang, *Nat. Commun.* **2013**, *4*, 2182; b) M. P. Cecchini, V. A. Turek, J. Paget, A. A. Kornyshev, J. B. Edel, *Nat. Mater.* **2013**, *12*, 165 – 171.
[15] H. Ortner, *Fresenius J. Anal. Chem.* **1992**, *343*, 695 – 704.
[16] M. Mulvihill, A. Tao, K. Benjauthrit, J. Arnold, P. Yang, *Angew. Chem.* **2008**, *120*, 6556 – 6560; *Angew. Chem. Int. Ed.* **2008**, *47*, 6456 – 6460.
[17] a) J. A. Dieringer, A. D. McFarland, N. C. Shah, D. A. Stuart, A. V. Whitney, C. R. Yonzon, M. A. Young, X. Zhang, R. P. Van Duyne, *Faraday Discuss.* **2006**, *132*, 9 – 26; b) P. K. Jain, W. Huang, M. A. El-Sayed, *Nano Lett.* **2007**, *7*, 2080 – 2088.
[18] P. Larkin, *Infrared and Raman Spectroscopy; Principles and Spectral Interpretation*, Elsevier Science, Amsterdam, **2011**.
[19] a) M. Chen, I. Y. Phang, M. R. Lee, J. K. W. Yang, X. Y. Ling, *Langmuir* **2013**, *29*, 7061 – 7069; b) B. Sturman, E. Podivilov, M. Gorkunov, *Europhys. Lett.* **2013**, *101*, 57009.

